Supplementary Material for

Br$_2$ induced oxidative pore modification of a porous coordination network

Hiroyoshi Ohtsu*[a] and Masaki Kawano*[ab]

[a] *The Division of Advanced Materials Science, Pohang University of Science and Technology (POSTECH), RIST Building 3-3390, 77 Cheongam-Ro, Nam-Gu, Pohang, South Korea*

[b] *Department of Chemistry, Graduate School of Science and Engineering, Tokyo Institute of Technology, 2-12-1 Ookayama, Meguro-ku, Tokyo 152-8550, Japan*

* To whom correspondence should be addressed.

E-mail: mkawano@postech.ac.kr (MK), hotsu@postech.ac.kr (HO)

Experimental Details

Materials

TPT[10] and network $[(ZnI_2)_3(TPT)_2]_n$ (**1**)[9] were prepared according to the method described in the literature. All other chemicals and reagents were used as received.

Methods

High quality powder X-ray diffraction data for ab initio powder structure analyses were collected at SPring-8 BL02B2 (Japan). Powder X-ray diffraction data were collected on a Bruker D8 ADVANCE instrument in-house using reflection mode. IR spectra were recorded on a Varian 670-IR FT-IR spectrometer by the ATR method. Raman spectra were acquired by an inVia Raman microscope (Renishaw) with 830 nm wavelength excitations. UV/vis/NIR spectra were recorded on a Shimadzu UV/Vis-NIR scanning spectrophotometer UV-3600 using the diffuse-reflectance method for solid and the absorption method for solution. Thermogravimetric (TG) analysis was carried out at a ramp rate of 5 K/min in a nitrogen flow (30 ml/min. or 50 ml/min.) with a Setaram Labsys Evo instrument. Elemental analyses were performed on an Elementar vario MICRO cube at Technical Support Centre in Pohang University of Science and Technology.

Caution!!

Bromine is highly toxic; therefore, care must be taken to deal with it.

Bromine Exposure to Network 1, $[(ZnI_2)_3(TPT)_2]$:

Formation of I_2 encapsulating Porous Coordination Network $[(ZnBr_2)_3(TPT)_2(I_2)](I_2)_{0.67}$ (I_2@network 2)

In a glass container, 222.5 mg (0.141 mmol) of network **1** and 24.6 μl (0.478 mmol) of Br_2 were put separately (Figure S6). The glass container was capped by glass and left for ~ 1

minute until the yellow powder turned to reddish brown. The resulting powder (212 mg, yield 87%) was collected and analysed by XRPD and elemental analysis. We did not remove the surface I_2 produced by the reaction because washing or evacuating of the powder change the phase.

Elemental analysis:

Found: C, 25.10; H, 1.58; N, 9.73.

Calc. for $C_{36}H_{24}Br_6I_{3.34}N_{12}Zn_3$: $\{[(ZnBr_2)_3(TPT)_2(I_2)](I_2)_{0.67}\}$: C, 25.08; H, 1.40; N, 9.75%.

We assume the presence of surface I_2 on the crystalline powder because we did not perform any treatment to remove I_2 formed by reaction. The overall structure, $\{[(ZnBr_2)_3(TPT)_2(I_2)](I_2)_{0.67}\}$, determined from elemental analysis (24.6% of iodine) matched well with the TG data (25.3 % of I_2, see Figure S7).

Heating of I_2@network 2

Preparation of Porous Coordination Network, $[(ZnBr_2)_3(TPT)_2]$ (network 2)

180 mg (0.104 mmol) of I_2@network **2** was heated at 673 K under argon overnight (~ 10 h). The powder turned from reddish brown to off-white. The resulting powder (104 mg, yield, 77 %) was analysed by XRPD and elemental analysis.

Elemental analysis:

Found: C, 31.50; H, 2.05; N, 12.18.

Calc. for $C_{36}H_{30}Br_6N_{12}O_3Zn_3$: $[(ZnBr_2)_3(TPT)_2(H_2O)_3]$: C, 31.93; H, 2.23; N, 12.41%.

Bromine exposure to network 2, [(ZnBr$_2$)$_3$(TPT)$_2$]:

Br$_2$ encapsulating Porous Coordination Network [(ZnBr$_2$)$_3$(TPT)$_2$(Br$_2$)] (Br$_2$@network 2)

In a glass container, 80.0 mg (0.0615 mmol) of network **2** and 10 μl (0.194 mmol) of Br$_2$ were put separately (the same set-up as Figure S6).   The glass container was capped by glass and left for ~ 1 minute until the powder turned to yellow. The resulting powder (73.7 mg, yield 82%) was analysed by XRPD and elemental analysis.

Elemental analysis:

Found: C, 28.84; H, 1.94; N, 11.13.

Calc. for C$_{36}$H$_{28}$Br$_8$N$_{12}$O$_2$Zn$_3$:   [(ZnBr$_2$)$_3$(TPT)$_2$(Br$_2$)(H$_2$O)$_2$]: C, 28.90; H, 1.89; N, 11.23.

Ab initio Structure Determination from XRPD.

  The XRPD pattern of I$_2$@network **2**, network **2**, Br$_2$@network **2** were indexed using the program DICVOL[13]. The structure determination was carried out by the simulated annealing method with the program DASH[14]. The Rietveld refinements were performed with programs RIETAN-FP[16] and VESTA[17]. Restraints but no constraints for all bond lengths were employed to maintain the molecular geometry. Thermal temperature factors were refined isotropically and uniform values were applied to the framework and guest molecules. The details of the ab initio structure determinations are shown in 'Ab Initio crystal structure determination' section.

UV-vis. experiment in solution:

Kinetic Analysis of Bromine Exposure to network 1 in solution

Adsorption and pore modification experiments of Br$_2$ into network **1** were carried out at room temperature. A 0.48 mM Br$_2$ cyclohexane solution was prepared and 3mL of the solution (0.014 mmol) was transferred to a UV quartz cell (1 cm). ~7.4 mg (0.0047 mmol) of network

1 was put into the cell and the UV-Vis spectral change was measured at each 4 min. The selected spectra were shown in Figure S1.   The details of kinetic analyses were described in 'Adsorption kinetics' section.

Adsorption test of network 2 toward Br$_2$/I$_2$

Adsorptions of Br$_2$ and I$_2$ into network **2** were carried out at room temperature.   A 0.24 mM I$_2$ and Br$_2$ cyclohexane solution was prepared and 3mL of the solution was transferred to a UV quartz cell (1 cm).   ~9.9 mg of network **2** was put into the cell and the UV-Vis spectral change was measured at each 4 min for I$_2$ and at 3 min for Br$_2$.   The selected spectra were shown in Figure S11.   We could not determine adsorption kinetics for these experiments because cyclohexane compete the adsorption processes.

Adsorption kinetics

In the case of adsorption kinetics, the rate of adsorption can be determined from the following equation depending on the order of reaction[20]:

In the case of a first-order model,

$$d(q_t)/dt = k_1(q_e-q_t) \tag{1}$$

$$\ln(q_e-q_t) = \ln q_e - k_1 t \tag{2}$$

where, q_t : amount adsorbed at time (t) (mg/g), q_e: amount adsorbed at equilibrium (mg/g), k_1: pseudo-first-order kinetic constant (min^{-1})

In the case of a second-order model,

$$d(q_t)/dt = k_1(q_e-q_t)^2 \tag{3}$$

$$t/q_t = 1/(k_2 q_e^2)+t/q_e \tag{4}$$

where, k_2: pseudo-second-order kinetic constant (g/(mg•min))

In this I_2 adsorption case, q_t can be described by absorption:

$$q_t = (A_0-A_t)\times(1/\varepsilon)\times V_{cell}\times M_w(guest)\times(1/x) \tag{5}$$

where A_0: absorbance of the initial state, A_t: absorbance at time t, ε: molar absorption coefficient of guest, V_{cell} : volume of a solution (now 3 mL), M_w(guest): molecular weight of a guest molecule, x: amount of sorbent (network)

Therefore, in this case,

the plot of time vs. $\ln(A_t-A_\infty)$ is linear for the first-order reaction, and that of time vs. time/(A_0-A_t) is linear for the second-order. (A_∞: absorbance at equilibrium)

In the case of the first-order reaction, from the gradient, the rate of reaction can be determined.
In the case of the second-order, from intercept, the rate of reaction can be determined.
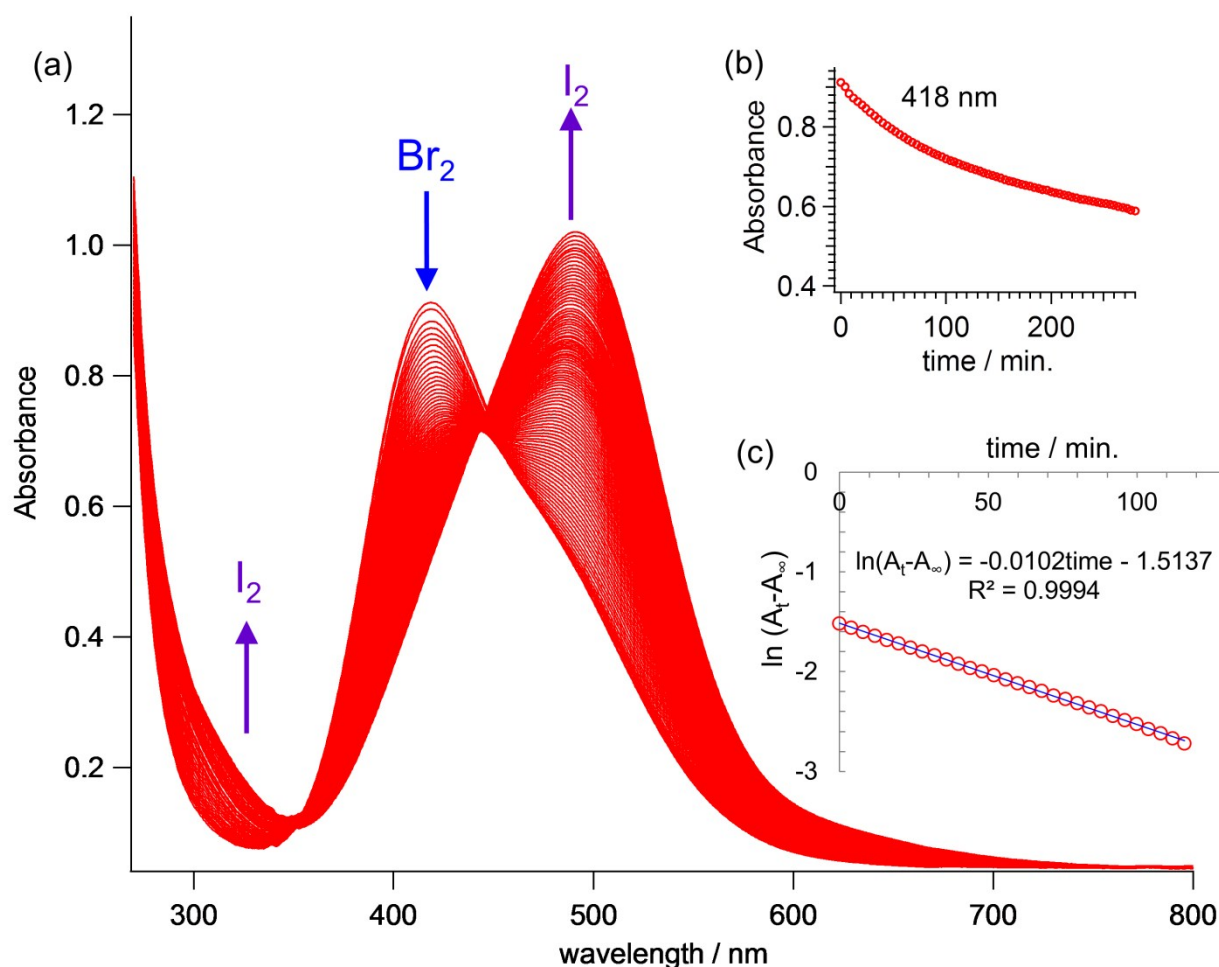
The details are shown below:

Pore modification reaction: Br$_2$ encapsulation into a pore

We simplified that this reaction is a simple adsorption process even though the reality is consecutive reactions.   In this case, this is a first-order reaction as shown in the inset of Figure S1.   The fitting curve is

$\ln(A_t-A_\infty) = -0.00102 \times \text{time} - 1.514$ ($R^2 = 0.999$)

Therefore, $k_1 = 1.0 \times 10^{-3}$ (min^{-1})

Figure S1. (a) Time-dependent UV-Vis. spectra of a Br$_2$ cyclohexane solution after the addition of network **1**. (b) The change in the absorbance at 418 nm with time. (c) Fitting with pseudo-first order kinetics (circles: observed data; line: fitted curve).

Ab Initio crystal structure determination

Ab initio crystal structure determination of [(ZnBr$_2$)$_3$(TPT)$_2$(I$_2$)] (I$_2$@network 2).
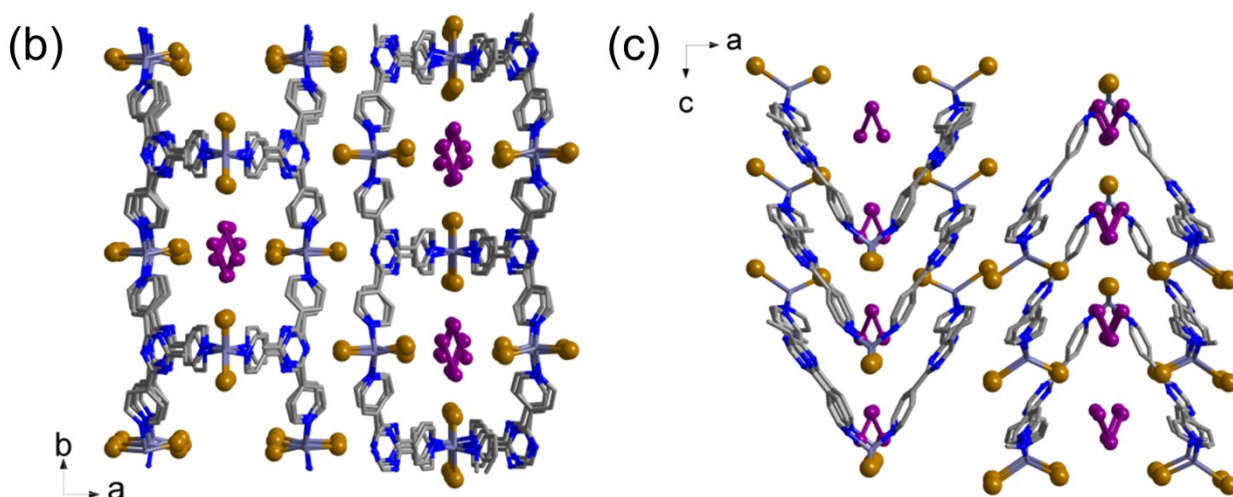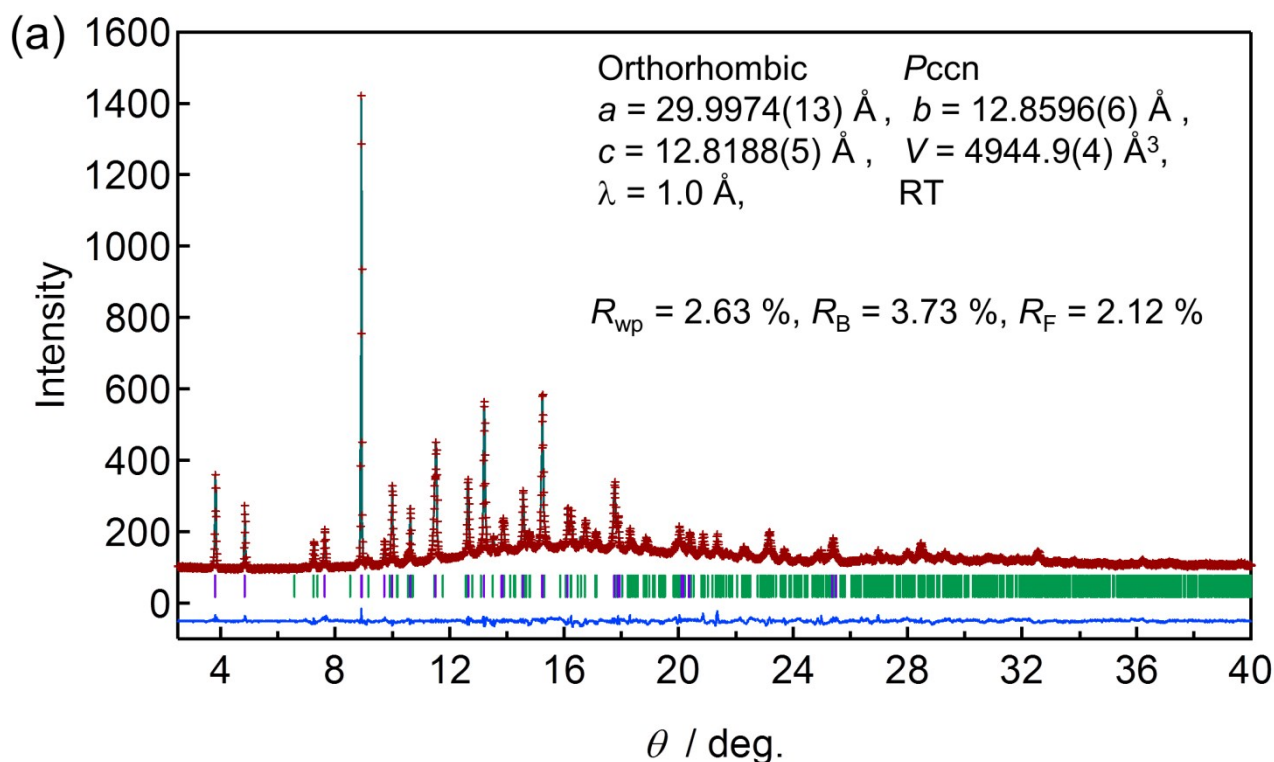
High quality powder X-ray diffraction pattern of I$_2$@network **2** was recorded at 298 K in transmission mode [0.3 mm capillary; synchrotron radiation $\lambda = 1.0$ Å; 2θ range, 0.01 to 79.15°; step size, 0.01°; data collection time, 20 min] on a diffractometer equipped with a blue imaging plate detector at BL02B2 beam line, SPring-8.

The XRPD pattern of I$_2$@network **2** was indexed using the program DICVOL (Boultif, A.; Louër, D. *J. Appl. Crystallogr*. **1991**, *24*, 987-993) to give a orthorhombic unit cell ($a = 30.008$ Å, $b = 12.865$ Å, $c = 12.817$ Å, $V = 4948.028$ Å^3) with good Figure of merit.   The space group was assigned from systematic absences as *Pccn*.   Unit cell and profile refinement were carried out using the Pawley method, led to good fit ($\chi^2 = 2.19$) for these lattice parameters and space group.   Structure solution was carried out by the simulated annealing method with the program DASH (David, W. I. F.; Shankland, K; van de Streek, J; Pidcock, E; Motherwell, W. D. S.; Cole, J. C, *J. Appl. Crystallogr.,* **2006**, *39*, 910-915).   Two rigid groups; [(ZnBr$_2$)$_3$(TPT)$_2$] in which Zn-N$_{pyridyl}$ were allowed to rotate and I$_2$ molecule with 50% occupancy, in asymmetric unit and Z = 4 for space group *P*ccn were introduced by using a constrained Z-matrix description.   During annealing, 26 runs of 1×10^7 Monte Carlo moves each were performed.   The best structure obtained (Profile $\chi^2 = 8.18$) was taken as the starting structural model for Rietveld refinement.

The Rietveld refinement of I$_2$@network **2** was performed with the program RIETAN-FP (Izumi, F.; Momma, K. *Solid State Phenom.,* **2007**, *130*, 15-20) and VESTA (Momma, K.; Izumi, F. *J. Appl. Crystallogr.,* **2008**, *41*, 653-658).   Restraints but no constraints for all bond lengths were employed to maintain the molecular geometry.   Atomic displacement parameters were refined isotropically with uniform values for atoms composed of the network and different uniform values for I$_2$ guest atoms.

Final Rietveld refinement result: $a = 29.997(1)$ Å, $b = 12.8596(6)$ Å, $c = 12.8188(5)$ Å, V =

4944.9(4) Å^3, R_{wp} = 2.629% (R_e = 8.449%), R_p = 1.952%, R_B = 3.732%, R_F = 2.119%; 3751 profile

points (2θ range, 2.5 to 40°); 265 refined variables.   The result is shown in Figure S2.

Figure S2. (a) Experimental (red), calculated (black), and difference (blue) XRPD profiles from the final Rietveld refinement of the I$_2$@network **2**. Crystal structure: (b) view along the *c*-axis. I$_2$ (occupancy 0.5) occupies two symmetrically related positions. (c) View along the *b*-axis. Colour codes: C, grey; N, blue; Zn, pale-blue; I, purple; and Br, brown.
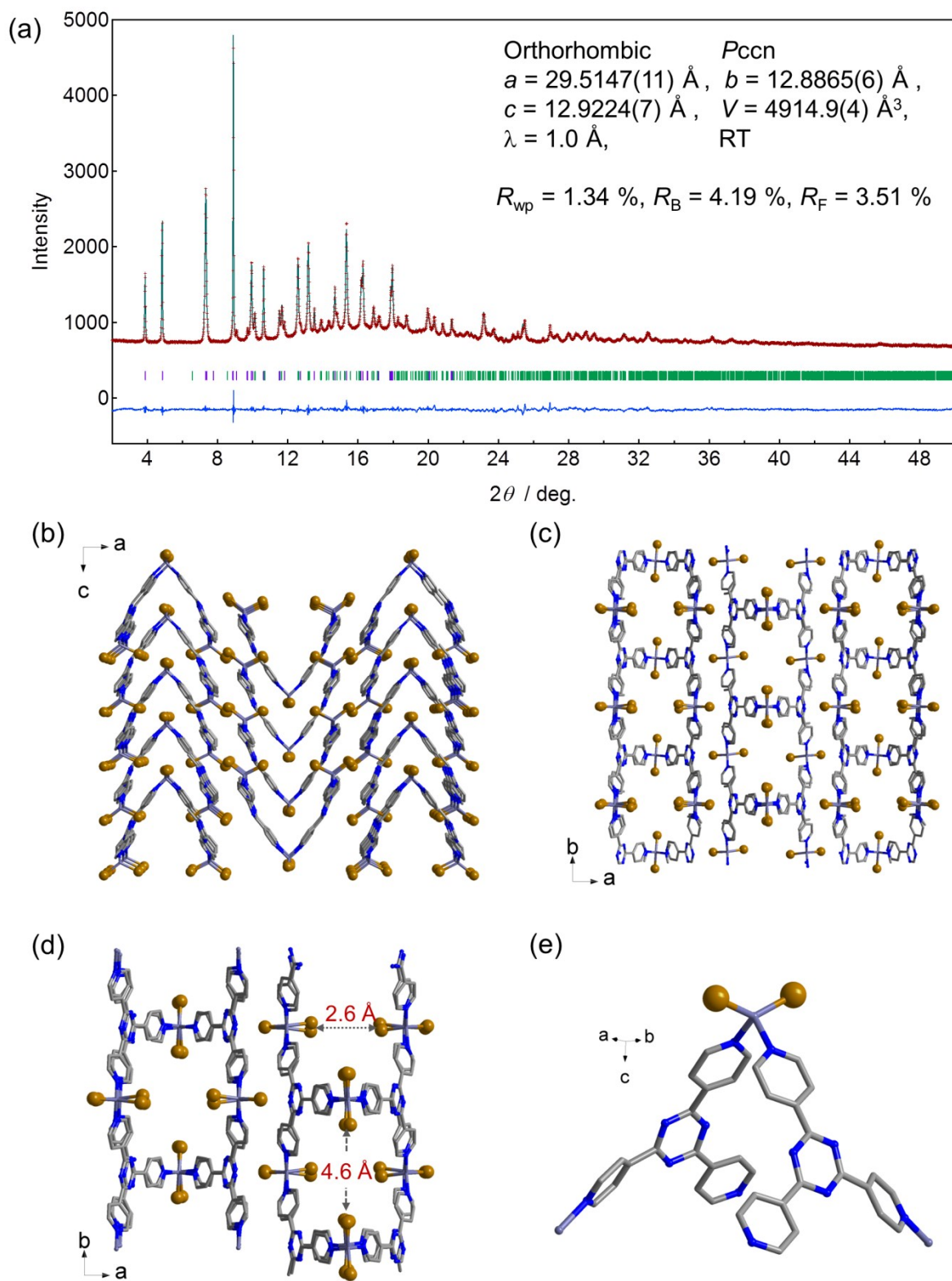
Ab initio crystal structure determination of [(ZnBr$_2$)$_3$(TPT)$_2$] (network 2).

High quality powder X-ray diffraction pattern of network **2** was recorded at 298 K in transmission mode [0.3 mm capillary; synchrotron radiation λ = 1.0 Å; 2θ range, 0.01 to 79.21°; step size, 0.01°; data collection time, 30 min] on a diffractometer equipped with a blue imaging plate detector at BL02B2 beam line, SPring-8.

The XRPD pattern of network **2** was indexed using the program DICVOL (Boultif, A.; Louër, D. *J. Appl. Crystallogr.* **1991**, *24*, 987-993) to give a orthorhombic unit cell (a = 29.559 Å, b = 12.897 Å, c = 12.918 Å, V = 4924.617 Å^3) with good Figure of merit.   The space group was assigned from systematic absences as *Pccn*.   Unit cell and profile refinement were carried out using the Pawley method, led to good fit (χ^2 = 7.28) for these lattice parameters and space group.   Structure solution was carried out by the simulated annealing method with the program DASH (David, W. I. F.; Shankland, K; van de Streek, J; Pidcock, E; Motherwell, W. D. S.; Cole, J. C, *J. Appl. Crystallogr.,* **2006**, *39*, 910-915).   One rigid group of [(ZnBr$_2$)$_3$(TPT)$_2$] in which Zn-N$_{pyridyl}$ were allowed to rotate, in asymmetric unit and Z = 4 for space group *P*ccn were introduced by using a constrained Z-matrix description.   During annealing, 26 runs of 1×10^7 Monte Carlo moves each were performed. The best structure obtained (Profile χ^2 = 11.13) was taken as the starting structural model for Rietveld refinement.

The Rietveld refinement of network **2** was performed with the program RIETAN-FP (Izumi, F.; Momma, K. *Solid State Phenom.*, **2007**, *130*, 15-20) and VESTA (Momma, K.; Izumi, F. *J. Appl. Crystallogr.*, **2008**, *41*, 653-658).   Restraints but no constraints for all bond lengths were employed to maintain the molecular geometry.   Atomic displacement parameters were refined isotropically with uniform values for atoms composed of the network.

Final Rietveld refinement result: a = 29.514(1) Å, b = 12.8865(6) Å, c = 12.9224(7) Å, V = 4914.9(4) Å^3, R_{wp} = 1.336% (R_e = 9.873%), R_p = 1.025%, R_B = 4.193%, R_F = 3.513%; 4801 profile points (2θ range, 2 to 50°); 303 refined variables.   The result is shown in Figure S3.

Figure S3. (a) Experimental (red), calculated (black), and difference (blue) XRPD profiles from the final Rietveld refinement of network **2**. Crystal Structure: (b) view along the *b*-axis. (c) View along the *c*-axis. (d) Pore description. (e) One unit of network **2**. Color codes: C, grey; N, blue; Zn, pale-blue; and Br, brown.

Ab initio crystal structure determination of [(ZnBr$_2$)$_3$(TPT)$_2$(Br$_2$)] (Br$_2$@network 2).

High quality powder X-ray diffraction pattern of Br$_2$@network **2** was recorded at 298 K in transmission mode [0.3 mm capillary; synchrotron radiation $\lambda = 1.0$ Å; 2θ range, 0.01 to 79.14°; step size, 0.01°; data collection time, 40 min] on a diffractometer equipped with a blue imaging plate detector at BL02B2 beam line, SPring-8.

The XRPD pattern of Br$_2$@network **2** was indexed using the program DICVOL (Boultif, A.; Louër, D. *J. Appl. Crystallogr*. **1991**, *24*, 987-993) to give a orthorhombic unit cell ($a = 29.362$ Å, $b = 12.835$ Å, $c = 12.859$ Å, b = 91.198°, $V = 4845.299$ Å^3) with good Figure of merit. The space group was assigned from systematic absences as $P2_1/n$. Unit cell and profile refinement were carried out using the Pawley method, led to good fit ($\chi^2 = 13.60$) for these lattice parameters and space group. Structure solution was carried out by the simulated annealing method with the program DASH (David, W. I. F.; Shankland, K; van de Streek, J; Pidcock, E; Motherwell, W. D. S.; Cole, J. C, *J. Appl. Crystallogr.,* **2006**, *39*, 910-915). Three rigid groups; [(ZnBr$_2$)$_3$(TPT)$_2$] in which Zn-N$_{pyridyl}$ were allowed to rotate and two Br$_2$ molecule with 50% occupancy, in asymmetric unit and Z = 4 for space group $P2_1/n$ were introduced by using a constrained Z-matrix description. During annealing, 26 runs of 1×10^7 Monte Carlo moves each were performed. The best structure obtained (Profile $\chi^2 = 4.37$) was taken as the starting structural model for Rietveld refinement.

The Rietveld refinement of Br$_2$@network **2** was performed with the program RIETAN-FP (Izumi, F.; Momma, K. *Solid State Phenom*., **2007**, *130*, 15-20) and VESTA (Momma, K.; Izumi, F. *J. Appl. Crystallogr*., **2008**, *41*, 653-658). Restraints but no constraints for all bond lengths were employed to maintain the molecular geometry. We also carefully investigated several possibilities of disordered Br$_2$. After the Rietveld refinement, the most reasonable model was found to be two disordered Br$_2$ which resulted in the minimum residual diffraction intensities. Atomic displacement parameters were refined isotropically with uniform values for Zn, C, N atoms composed of the network and refined with different uniform values for bromides and with another different uniform values for Br$_2$ guest atoms.

Final Rietveld refinement result: a = 29.3371(13) Å, b = 12.8766(8) Å, c = 12.8601(8) Å, β = 90.952(4) °, V = 4857.4(5) Å^3, R_{wp} = 2.098% (R_e = 5.964%), R_p = 1.431%, R_B = 2.418%, R_F = 1.287%; 3781 profile points (2θ range, 2.2 to 40°); 346 refined variables.   The result is shown in Figure S4.
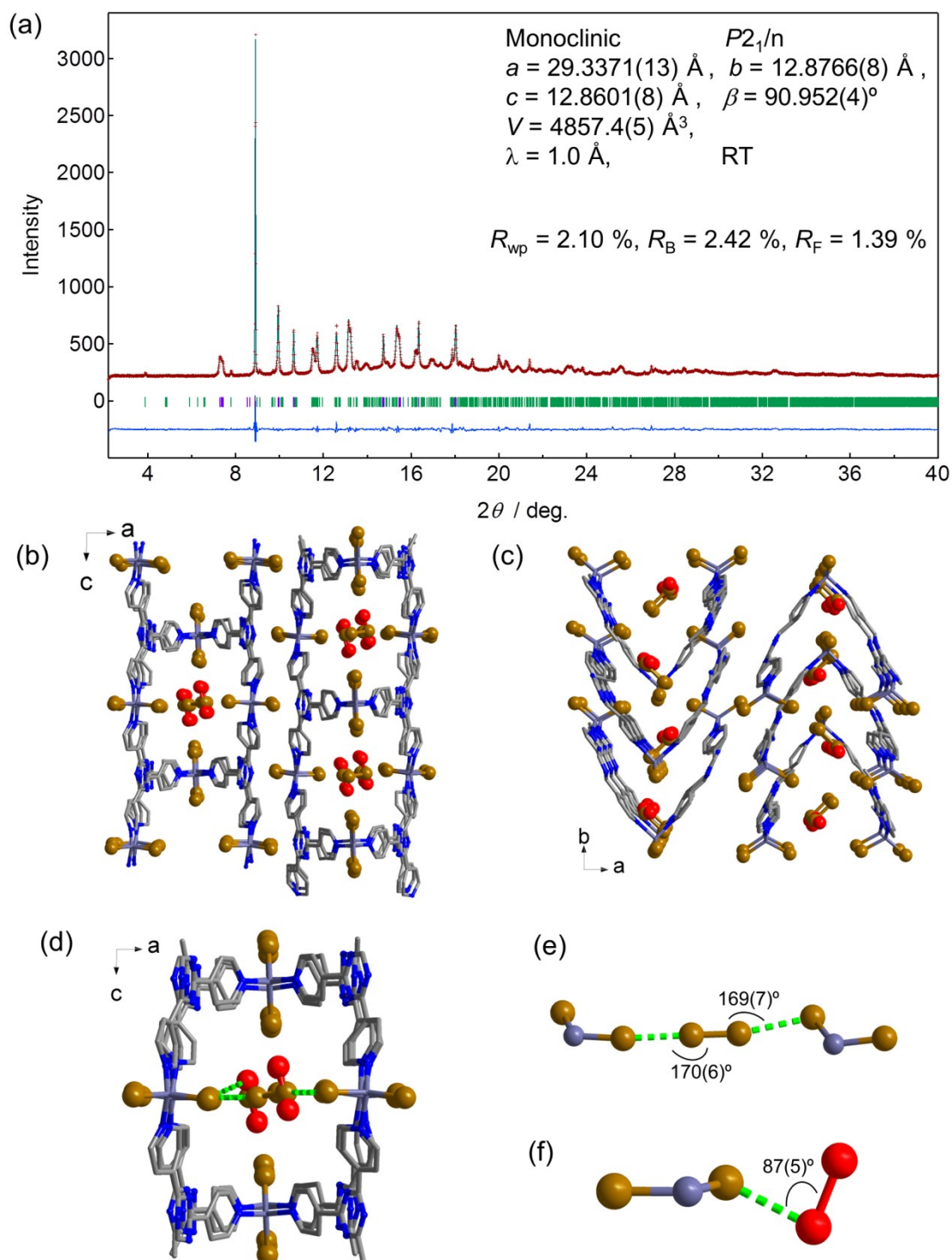
Figure S4. (a) Experimental (red), calculated (black), and difference (blue) XRPD profiles from the final Rietveld refinement of Br_2@network **2**. Crystal Structure: (b) view along the *b*-axis. (c) View along c-axis. (d) Pore description with interaction between Br_2 and bromide (green dotted line). (e) Linear interactions between Br_2 and Br^- ions. (f) Perpendicular interactions between Br_2 and Br^- ions. Color codes: C, grey; N, blue; Zn, pale-blue; Br, brown and red (disorder).
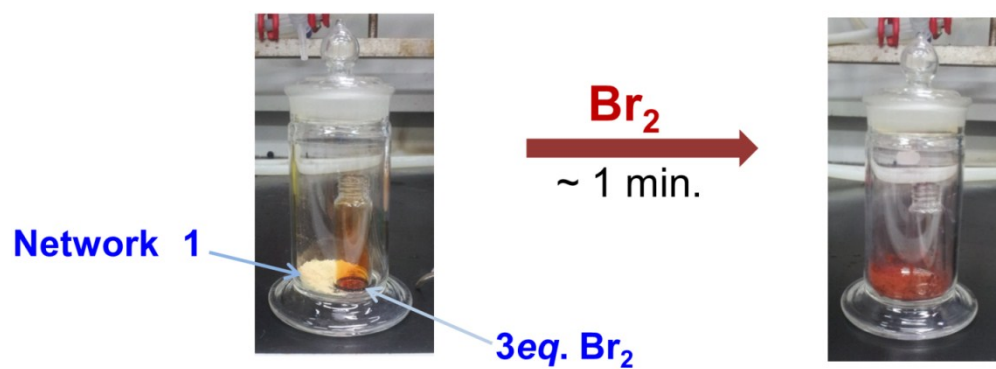
Structure of network 1, [(ZnI$_2$)$_3$(TPT)$_2$]$_n$
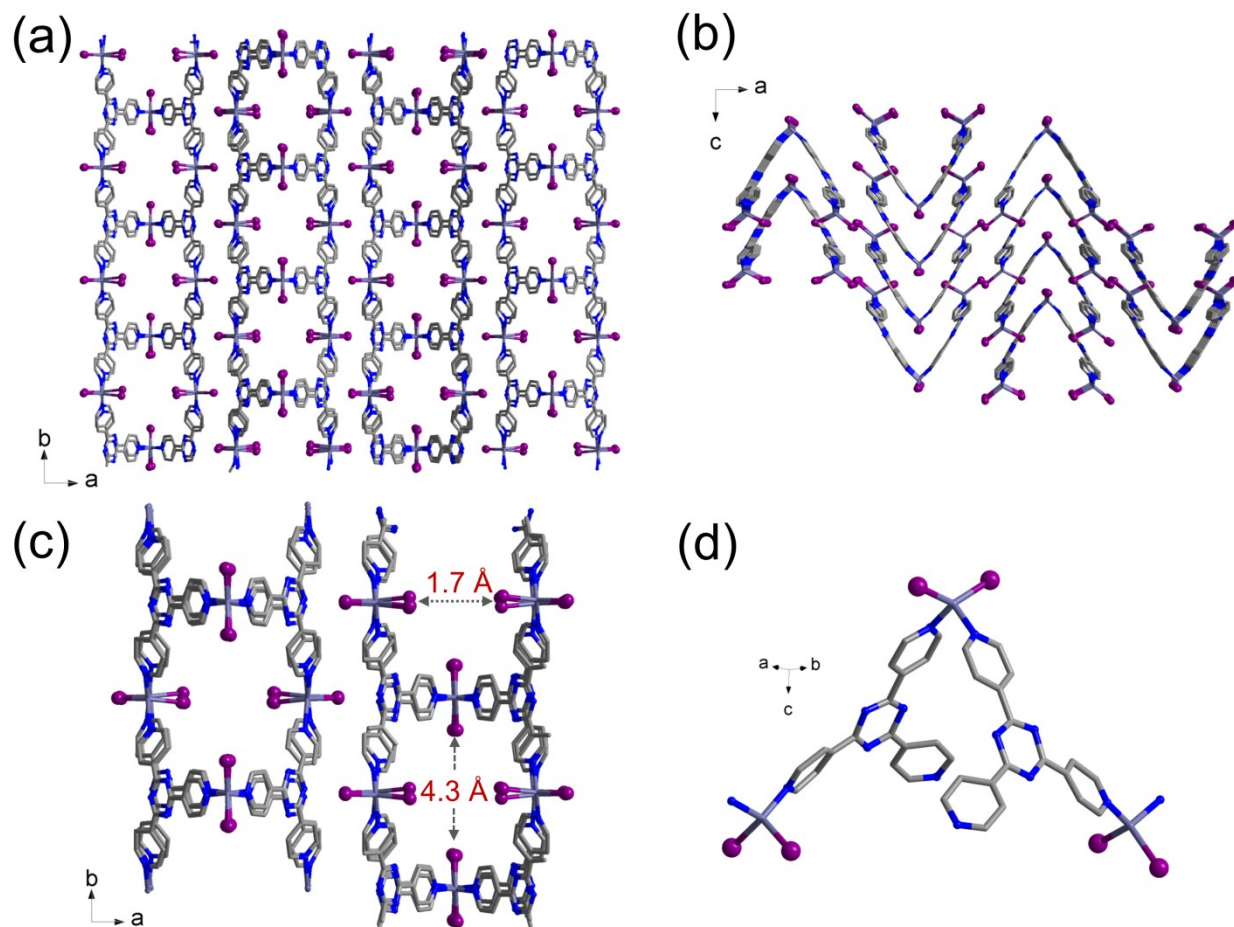
Figure S5. Crystal structure of network **1**, [(ZnI$_2$)$_3$(TPT)$_2$]$_n$, (a) the *c*-axis projection, (b) the *b*-axis projection, (c) pore view from *c*-axis, (d) view of one saddle type unit, Colors: Zn, thin-purple ; I, purple, C, grey, N, blue.   Hydrogen atoms are omitted for clarity.
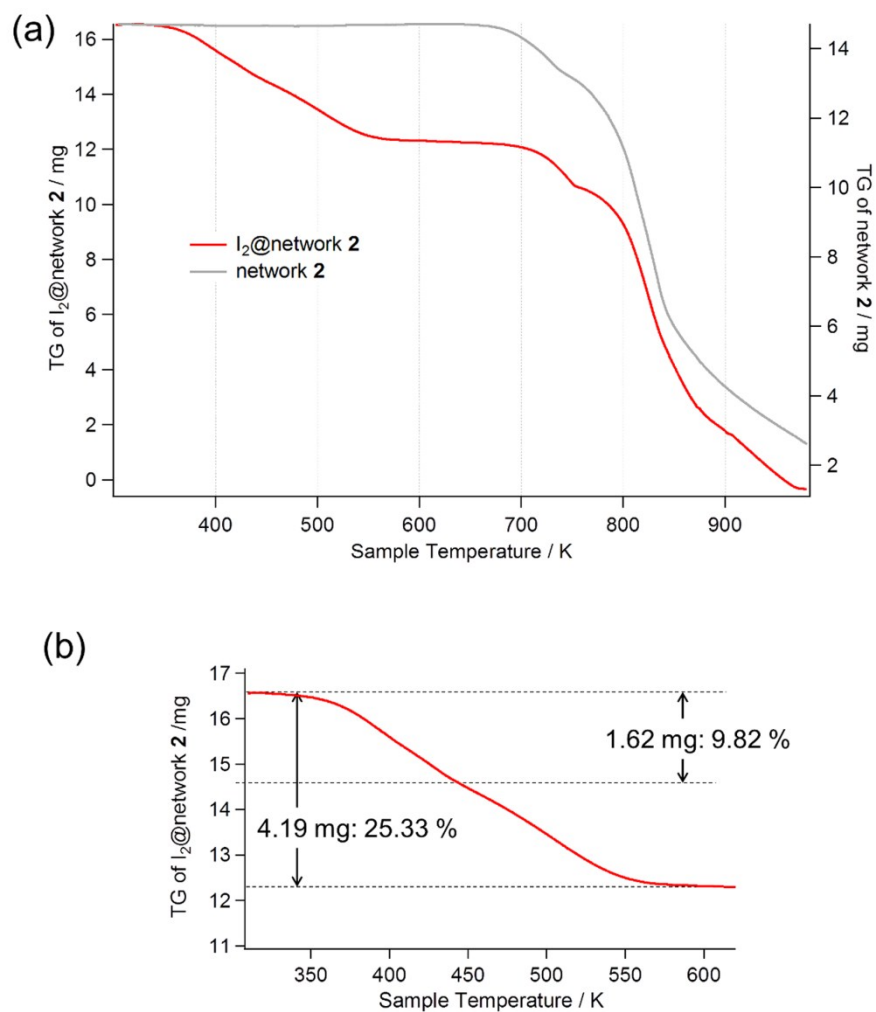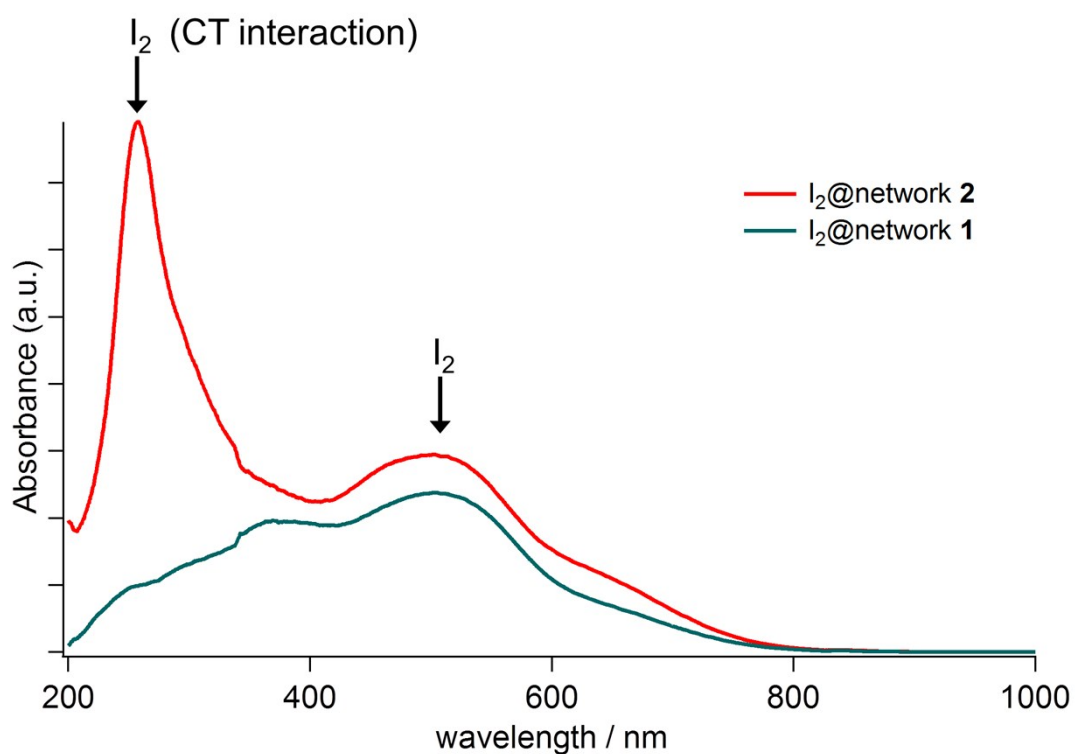
Experimental Set-up of Br₂ exposure

Figure S6. Experimental set up of Br$_2$ vapor exposure to network **1**.

TG of network 2 and I$_2$@network 2


Figure S7. (a) TG of I$_2$@network **2** and network **2** (b) TG of I$_2$@network **2** shows two steps weight decreases: the first step corresponds to surface I$_2$ and the second step corresponds to I$_2$ in the pore.

Solid-State UV-Vis. Spectra

Figure S8. Diffuse-reflectance UV-Vis-NIR spectra of I$_2$@network **2** and I$_2$@network **1**. Absorbance was calculated by Kubelka-Munk transformation.   I$_2$ peaks were observed at 532 nm for both networks.   In the case of I$_2$@network **2**, the typical charge transfer transition was observed at 280 nm, which indicates strong interaction between pore Br$^-$ and I$_2$.

IR spectra
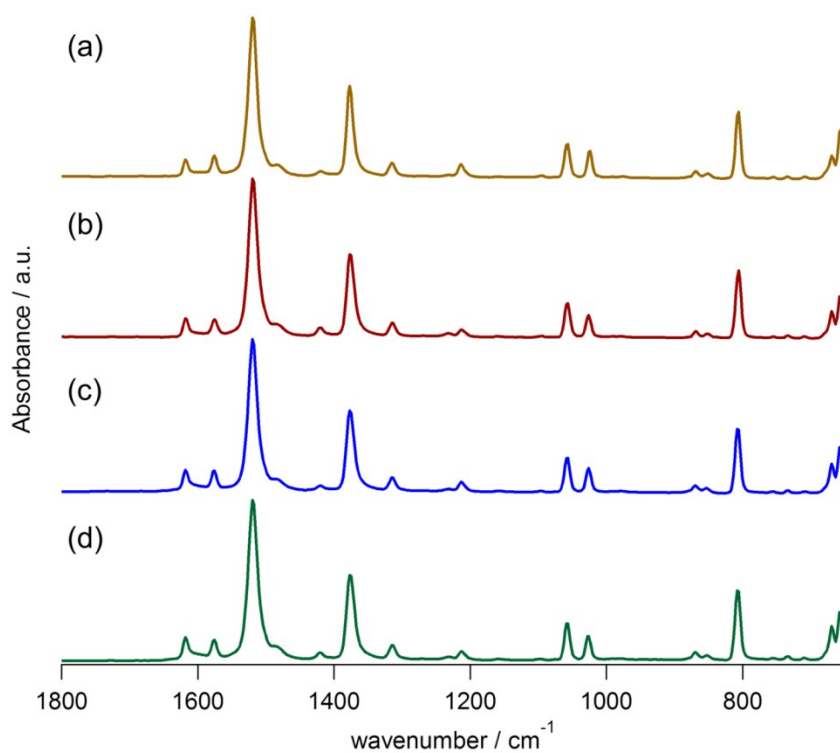
Figure S9. IR spectra of (a) network **1**, (b) I_2@network **2**, (c) network **2**, (d) Br_2@network **2**. Every IR spectrum is similar as each other because the peaks in this range mainly are attributed to TPT ligand.

Raman spectra
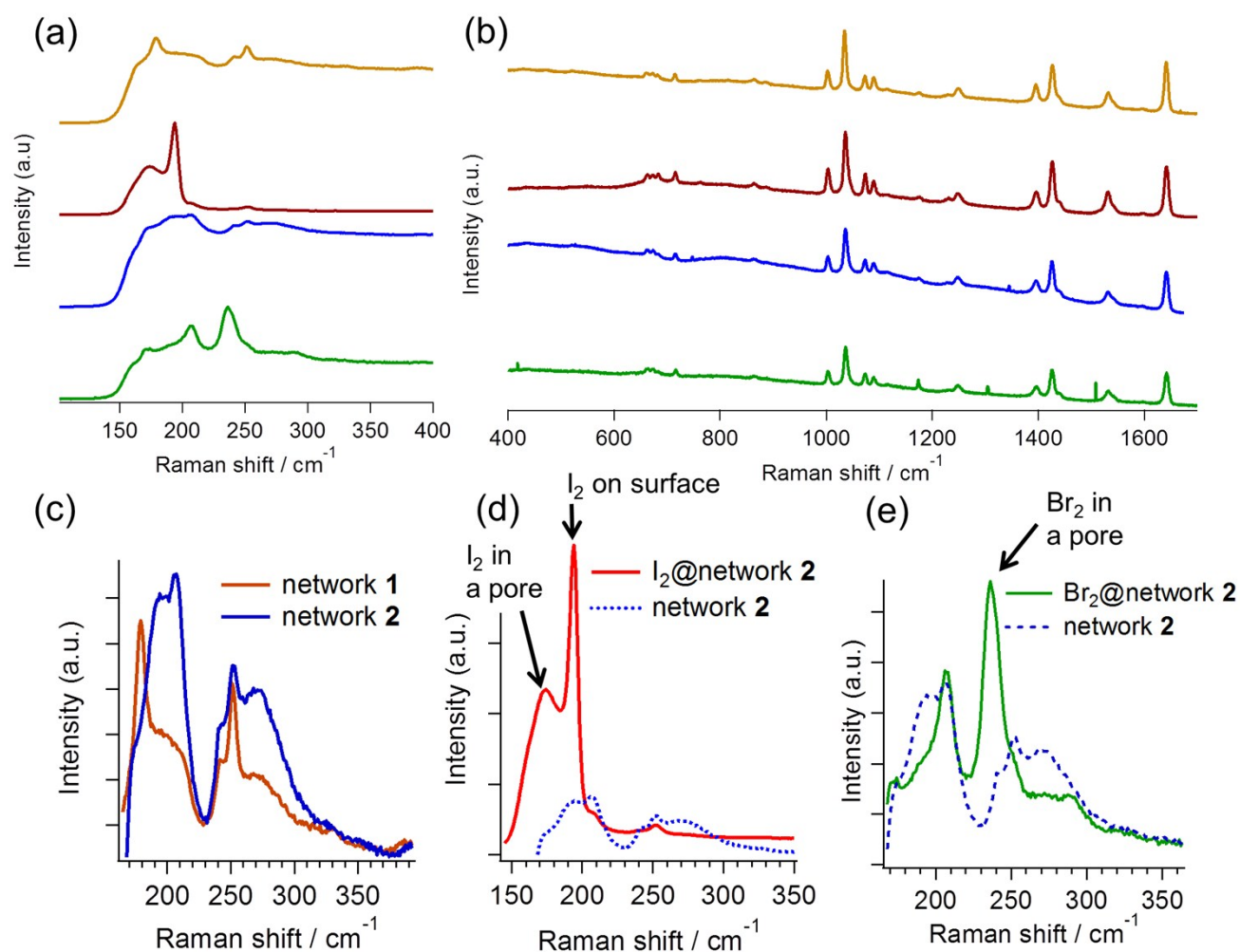
Figure S10. Non-scaled Raman spectra of network **1** (dark yellow), I_2@network **2** (brown), network **2** (blue), and Br_2@network **2** (green) for the range of (a) 100-400 cm^{-1} and (b) 400-1700 cm^{-1}. Scaled Raman spectra at the low wavenumber region of (c) network **1** and **2**, (d) I_2@network **2** and network **2**, (e) Br_2@network **2** and network **2**.

The Raman spectrum of network **2** shows the significant difference from that of network **1** in the low wavenumber region; while network **1** shows 179 cm^{-1} of Zn-I band, network **2** shows 208 cm^{-1} of Zn-Br band. Both of the networks have peaks in 240-270 cm^{-1} of Zn-N bands.

Adsorption test of network 2 toward I$_2$/Br$_2$
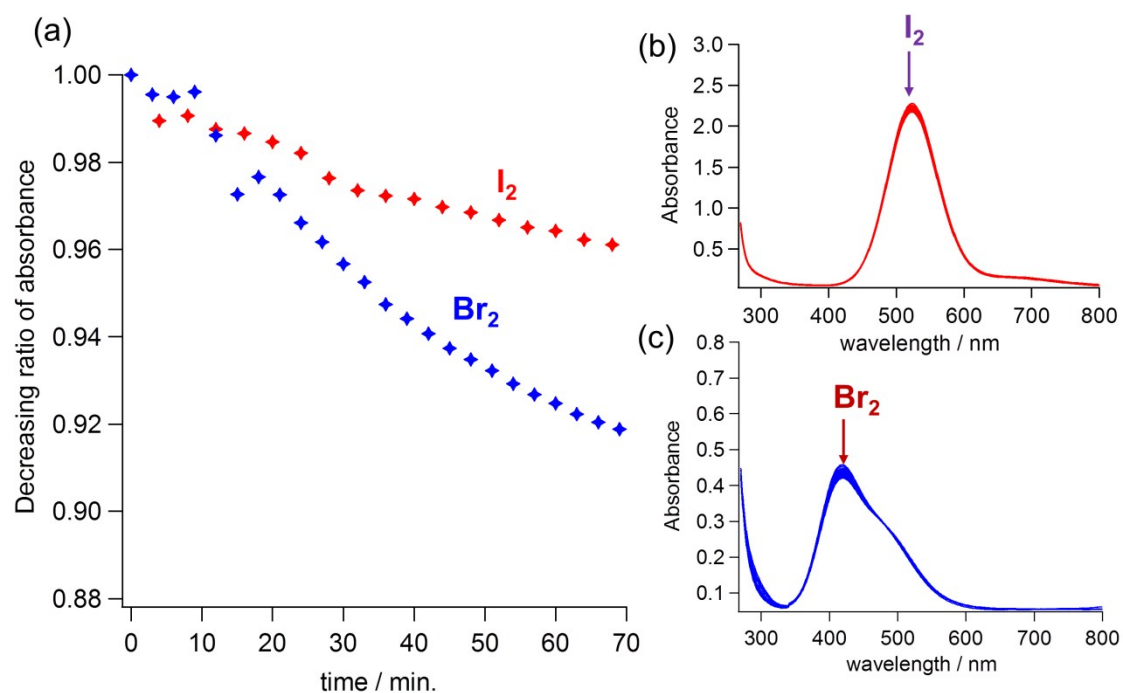
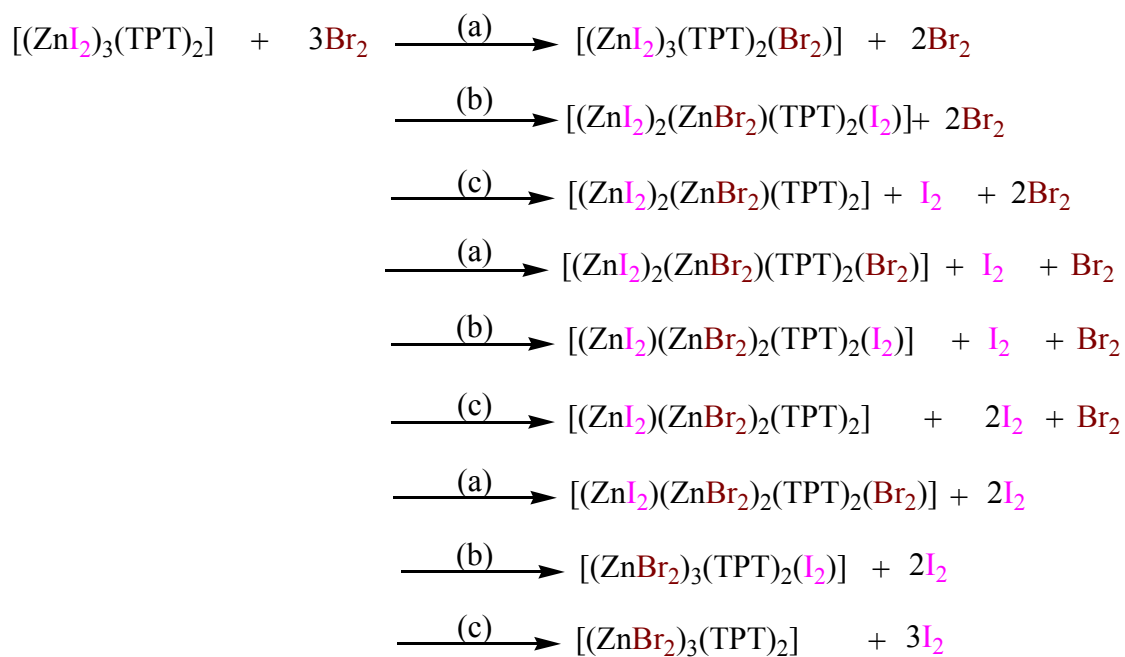**Figure S11.** Adsorption kinetics of network **2** with I$_2$/Br$_2$. (a) The decreasing ratio of absorbance depending on time after putting network **2** into I$_2$/Br$_2$ solution: red shows the case of I$_2$ solution using absorption at 523 nm, blue shows the case of Br$_2$ solution using absorption at 418 nm. In both cases, the ratio at 0 min. was set to 1. (b) Time dependent UV-Vis. spectra of I$_2$ cyclohexane solution after putting network **2**. (c) Time dependent UV-Vis. spectra of Br$_2$ cyclohexane solution after putting network **2**.

Complete chemical reaction scheme for pore modification in solution:

$$[(ZnI_2)_3(TPT)_2] \ + \ 3Br_2 \ \xrightarrow{(a)} \ [(ZnI_2)_3(TPT)_2(Br_2)] \ + \ 2Br_2$$

$$\xrightarrow{(b)} \ [(ZnI_2)_2(ZnBr_2)(TPT)_2(I_2)] + \ 2Br_2$$

$$\xrightarrow{(c)} \ [(ZnI_2)_2(ZnBr_2)(TPT)_2] \ + \ I_2 \ + \ 2Br_2$$

$$\xrightarrow{(a)} \ [(ZnI_2)_2(ZnBr_2)(TPT)_2(Br_2)] \ + \ I_2 \ + \ Br_2$$

$$\xrightarrow{(b)} \ [(ZnI_2)(ZnBr_2)_2(TPT)_2(I_2)] \ + \ I_2 \ + \ Br_2$$

$$\xrightarrow{(c)} \ [(ZnI_2)(ZnBr_2)_2(TPT)_2] \ + \ 2I_2 \ + \ Br_2$$

$$\xrightarrow{(a)} \ [(ZnI_2)(ZnBr_2)_2(TPT)_2(Br_2)] \ + \ 2I_2$$

$$\xrightarrow{(b)} \ [(ZnBr_2)_3(TPT)_2(I_2)] \ + \ 2I_2$$

$$\xrightarrow{(c)} \ [(ZnBr_2)_3(TPT)_2] \ + \ 3I_2$$

One process consists of three steps:

(a) Br_2 diffusion into a pore

(b) Pore modification by oxidation reaction

(c) I_2 desorption into solution

TOPOS Analysis Result of network 2 (the same as network 1)

Point symbol for net: {4^2.6}

3-c net; uninodal net

You have to increase Max.Ring value to compute plane net VS correctly!

Topological type: SP 1-periodic net (4,4)(0,2) (1D_2D.ttd) {4^2.6} - VS [4.4.*] (76179 types in 11 databases)